

# Pulsar electrons detection in AMS-02 experiment. Model status and discovery potential.

Jonathan Pochon\*

*Instituto de Astrofísica de Canarias, C. Vía Láctea, 38200, La Laguna, Tenerife, Spain*

December 10, 2009

## Abstract

The measurements of electrons ( $e^\pm$ ) from cosmic ray events have begun a new era a few years ago with high precision experiments like PAMELA [1] and Fermi-LAT [2]. The positron fraction seems to indicate an unknown component above the standard background described in the last 40 years mostly by HEAT [3]. In the last few years, the PAMELA satellite has confirmed the positron fraction excess above 10 GeV. In the case of Fermi-LAT data, the electron flux is steeper than expected. While these new measurements have not closed the debate, results from AMS-02 [4] are expected to reach the accuracy needed to determine a full description of this excess and possibly give some evidence on the possible source. We will present in this note, the AMS-02 capacity in the case of positrons produced by pulsars.

## Introduction

The context of the positron-electron cosmic rays can be summarized by a series of measurements in disagreement with what we understand. Indeed, since the 70s most of the experiments, namely TS93 [5], HEAT [6] [7], Caprice [8], AMS-01 [9], PAMELA [10], exhibit a deviation from the standard framework in the positron fraction ( $\frac{e^+}{e^++e^-}$ ), represented by figure 1 (left). Looking at the total flux of  $e^\pm$ , observations by Fermi-LAT [11], balloon experiments like ATIC [12] and ground ones like HESS [13] present a steeper behavior summarized in figure 1 (right). The standard propagation model can well explain the cosmic rays energy spectrum above 1 GeV, shown in studies by Moskalenko and Strong [14]. However, the positron fraction above 10 GeV remains unexplained. All models from propagation to source candidates were improved trying to reproduce observational data. During propagation, most of the models are consistent between them, the data uncertainty allowing high degeneracy models [15], in particular for the measurement of the nuclei ratio  $B/C$ ,  $Be^9/Be^{10}$ . Regarding source candidates, two approaches seem to be preferred. The first one, is to consider the closest astrophysical objects able to produce positron-electron pairs, like e.g. pulsars [16] [17]. Some pulsars are sufficiently close and energetic to be responsible of positrons deviation. The second

---

\*email: jgpoochon@iac.es

possibility, is to consider dark matter particles, which can produce  $e^\pm$  through annihilation [18] [19] or decaying [20]. So far, only PAMELA and ATIC have claimed or confirmed such a deviation from standard background. For PAMELA (figure 1 left) the positron fraction above 10 GeV is growing, while for ATIC, the electron flux forms a "bump" around 400 GeV (figure 1 right). However, the Fermi-LAT measurements do not agree with the ATIC bump result, establishing only a mildly harder  $e^\pm$  flux [21]. In this context, AMS-02 will be a powerful detector able to give crucial informations on positrons that are directly connected to this possible extra contribution with respect to expected background. This note will discuss the topic of electrons produced by pulsars, and will present the AMS-02 capacity.

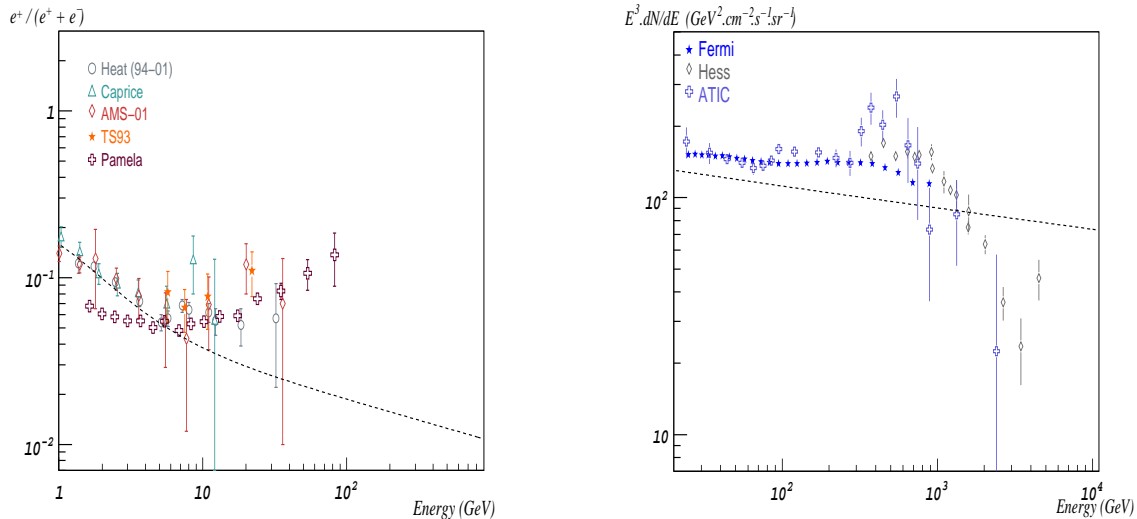


Figure 1: *Left: Positron fraction for TS93 [5], HEAT [6] [7], Caprice [8], AMS-01 [9] and PAMELA [10] compared with expected background [14]. Right: Electrons flux for Fermi-LAT, HESS and ATIC compared to the standard background.*

## 1 Electrons coming from pulsars

Since the discovery of pulsars in 1967 [22], most of the models agree with measurements like periodicity, but some unknowns still remain, e.g. the gamma-ray production. Electron production in the pulsar has not yet been observed, and their detection would be an interesting discovery. Through systematic surveys, pulsars are well studied and basic characteristic are available. Figure 2 (left) shows that for the Australia Telescope National Facility (ATNF) [23], observed pulsars in the Galaxy cover a good range in distance.

### 1.1 Pulsar $e^\pm$ production

Gamma-ray production in pulsars, giving electron-positron pairs, can be modeled by two mechanisms of relativistic particle acceleration: the *polar cap* (PC) [24] [25] and the *outer gap* (OG) [26]. EGRET [27] [28] has shown evidence, for several pulsars, of a pulsed gamma-ray emission at GeV scale, giving confidence to the fact that the magnetosphere must be involved for the charged particle acceleration.

P. Goldreich and W.H. Julian [29] have demonstrated that magnetic field tears away electrons from the pulsar surface. The distribution of charged particles in the magnetosphere screens the electric field  $E_{\parallel}$  parallel to the magnetic field ( $\mathbf{B} \cdot \mathbf{E} = 0$ ), allowing the co-rotation of the whole system. But in some locations, the condition  $\mathbf{B} \cdot \mathbf{E} = 0$  is not maintained and particle can be accelerated following field lines. From there, a volume named *light cylinder* can be defined as a cylinder with the rotation axis as symmetry axis, and with radius equal to the co-rotating part. Outside this frontier, magnetic field lines are not closed. The acceleration can take place mostly in two locations. The first one is close to the surface near the magnetic pole, a situation described by the *polar cap* model (PC). The other, located between the last closed magnetic field line and the surface along the null electric surface defined by the condition  $\boldsymbol{\Omega} \cdot \mathbf{B} = 0$ , where  $\boldsymbol{\Omega}$  is the pulsar rotational velocity, a configuration dubbed the *outer gap* model (OG). Briefly, in both of them, quasi-static electric field accelerates the relativistic electrons, producing electron-positron pairs. The PC model consists of two steps. First one inside the acceleration region, a charged particle ( $e^{\pm}$ ) is taken away from the surface due to the electric field radiating gamma-ray by synchrotron. Then these gamma-rays create an  $e^{\pm}$  pair, through magnetic field or by interaction with thermal X-rays from the pulsar surface. These secondaries are moving toward the light cylinder and then can escape. On the other hand, the OG model proposes a pair production from photon-photon interaction.  $e^{\pm}$  follow field lines radiating gamma-rays which interact with low energy photons (X-rays, infrared) producing  $e^{\pm}$  pairs, and then able to escape outside the light cylinder. First difference between the two models is that the OG location is farther than the PC one, so more distant from the magnetic field giving harder flux, while the PC configuration has a bigger contribution at low energy. Chi et al. [30] estimate that these two models give comparable total energy output in  $e^{\pm}$ . A criterion for the OG existence is given by Zhang et al. [31] and implies that  $g$ , ratio between dimension of the OG and radius of the light-cylinder, should be less than one. The OG existence condition can be expressed as [31]

$$g = 5.5P^{26/51} B_{12}^{-4/7} < 1. \quad (1)$$

with  $P$  being the pulsar period in  $s$  and  $B_{12}$  the pulsar magnetic field in  $10^{12}$  G. Conventionally, pulsars with the condition  $g < 1$  are gamma-ray pulsars. The ATNF [23] compiled the most complete and updated pulsar catalogue[32], comprising 1794 pulsars, with 272 being of the "gamma-ray" type. Figure 2 (left) demonstrates that "gamma-ray" pulsars in that catalogue cover a good range of distances in the Galaxy, and of ages.

## 1.2 Characteristics of the pulsar electron emission

The measurement accuracy on rotation frequency ( $\Omega = 2\pi/P$  [Hz]) and frequency derivative give an estimation on the pulsar age. A pulsar can be modeled like a rotating neutron star with a dipolar magnetic field misaligned with its rotation axis, producing pulsed radiation from the magnetic poles. In this way, the electromagnetic energy comes from rotational energy following a braking law of  $\dot{\Omega} \propto -\Omega^3$ , implying an energy variation  $\dot{E} = I\Omega\dot{\Omega}$ , proportional to the moment of inertia  $I$ . The pulsar rotational velocity can be written as [33]

$$\Omega(t) = \frac{\Omega_0}{(1 + t/\tau_0)^{1/2}} \quad (2)$$

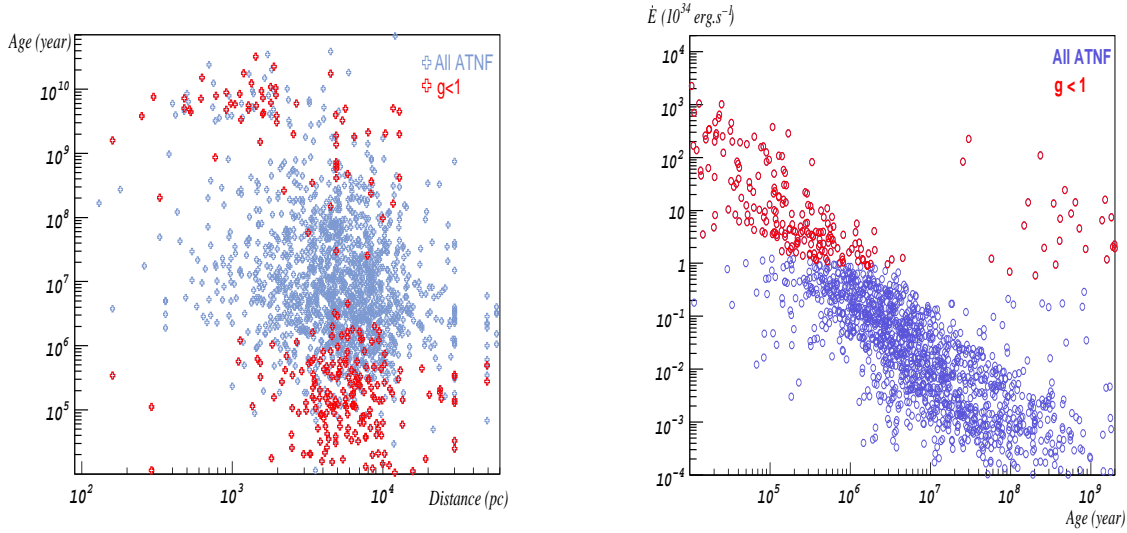


Figure 2: *Distribution of pulsars from the ATNF catalogue [23] including "gamma-ray" ones ( $g < 1$ ). Left: Pulsar age versus distance. Right: Pulsar spin-down power versus age.*

where  $\Omega_0$  is the initial spin frequency and  $\tau_0$  a decay time expressed as

$$\tau_0 = \frac{3c^3 I}{B^2 R_s^6 \Omega_0^2} \quad (3)$$

where  $I$  is the moment of inertia of the pulsar.  $\tau_0 \sim 10^4$  years for nominal parameters [34].  $\dot{E}$  is compared to the pulsar age in figure 2 (right), which establishes that the oldest objects have the lowest  $\dot{E}$ . At the same time, for each age sample, "gamma-ray" ones have the higher  $\dot{E}$ . Mature pulsars could contribute to  $e^\pm$  flux because produced particles are no longer trapped [30]. This framework allows us to derivate an estimated total released energy from a pulsar. Indeed, the upper limit to the rate of energy for electron-positron pairs is given by

$$\dot{E} = I\Omega\dot{\Omega} = \frac{1}{2}I\Omega_0^2 \frac{1}{\tau_0} \frac{1}{(1 + \frac{t}{\tau_0})^2} \quad (4)$$

From this equation, assuming an efficiency factor  $f_{e^\pm}$  for  $e^\pm$  pair production, the total energy that a mature pulsar ( $t \gg \tau_0$ ) has injected in magnetic dipole radiation is [35] [36]

$$E_{tot} \approx \frac{f_{e^\pm}}{2} I\Omega_0^2 \approx f_{e^\pm} \dot{E} \frac{T^2}{\tau_0} \quad (5)$$

where  $T$  is the typical age and  $\dot{E}$  the spin-down power. The expected value for the efficiency factor is  $f_{e^\pm} \sim \text{few } \%$  [35]. Other models, like Harding and Ramaty [37], Chi, Cheng and Young [38], and Zhang and Cheng [39], provide another  $E_{out}$  expression. As a consequence of energy losses from the source to the earth, the maximum energy of electrons reaching the observer is expressed as  $E_{max} = 3.10^3/t_5$  GeV, with  $t_5$  representing the electron age in  $10^5$  years unit. This implies that after  $10^5$  years, the maximum electron energy will be 3 TeV.  $E_{max}$  indicates the maximum reach by the pulsar electron spectrum. As a direct consequence, the oldest

the pulsar, the lowest is the  $E_{max}$ . Figure 3 (left) illustrates, for the whole ATNF catalogue, that  $E_{out}^{e^\pm}$  decreases with  $E_{max}$ , and that most of "gamma-ray" pulsars have a spectrum component above 10-100 GeV. Figure 3 (right) indicates that only three of the "gamma-ray" pulsars inside 1 kpc radius are able to contribute above 100 GeV.

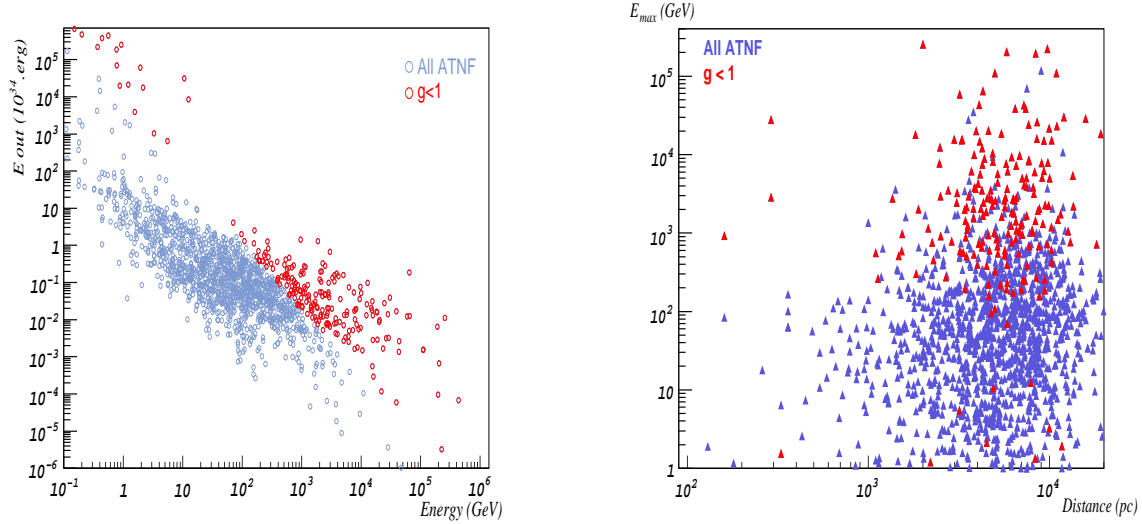


Figure 3: *Left: Standard pulsar  $E_{out}^{e^\pm}$  versus  $E_{max}$  reached. Right:  $E_{max}$  reached by pulsar versus pulsar distance.*

The spectral shape is limited at the energy range by  $E_{max}$  but also because  $e^\pm$  cannot be accelerated to arbitrarily high energies and a cut-off is expected around the TeV scale. Below that, we will assume a power law  $Q(E_e) \propto E^{-\alpha}$ . EGRET [27] [28] observations of galactic pulsars give a power index  $\alpha$  for gamma-ray spectra between 1.4 and 2.2. Assuming the power law measurement of cosmic electrons(positrons) of around 3.1 (3.3) [40], a pulsar contribution with enough intensity is expected to appear in the electron spectrum. Table 1 summarizes some properties for a sample of pulsars and one supernova, all of the objects being close enough and with a large spin-down energy loss, giving total energy released  $E_{tot}^{out}$ . In order to contribute above 10 GeV, these pulsars must be close-by ( $\sim 100$ -1000 pc) and their age must be less than  $60 \cdot 10^6$  years. Geminga and Monogem are the two most probable and/or popular sources for the positron fraction excess. The two are experimentally interesting because of the intensity and the spectrum range.

From this short-list, one can understand the importance of the energy range for the detector. Since pulsars can contribute from GeV to TeV scale, it is crucial to see a cut-off and/or decrease to validate the pulsar contribution. For example, PAMELA seems to be too low in energy to detect such cut-off, while AMS-02 and Fermi-LAT with their extended range up to TeV may detect it.

Table 1: *Data for selected nearby pulsars.*

| Name                 | Dist.<br>(pc) | Age<br>(years)    | g    | $E_{tot}^{out}$<br>( $10^{50}$ GeV) | $E_{max}$<br>(GeV) |
|----------------------|---------------|-------------------|------|-------------------------------------|--------------------|
| Geminga [J0633+1746] | 160.          | $3.42 \cdot 10^5$ | 0.70 | 74.                                 | 930.               |
| Monogem [B0656+14]   | 290.          | $1.11 \cdot 10^5$ | 0.14 | 9.                                  | 2850.              |
| Vela [B0833-45]      | 290.          | $1.13 \cdot 10^4$ | 0.70 | 17.                                 | 28040.             |
| B0355+54             | 1100.         | $5.64 \cdot 10^5$ | 0.61 | 281.                                | 562.               |
| Loop I [SNR]         | 170.          | $2 \cdot 10^5$    | -    | 43.                                 | 1584.              |

## 2 Flux at earth after propagation

### 2.1 Solution of diffusion equation

After production of  $e^\pm$ , these particles mostly lose energy by synchrotron radiation (SR) and inverse Compton scattering (ICS). Their motion depends on the galactic magnetic field, which enables the direction reconstruction for charged particles. These processes are calculated by solving the transport equation in the standard diffusion approximation (neglecting convection), which for local sources can be expressed with a spherical symmetry, and reduced to the form [41]

$$\frac{\partial}{\partial t} \frac{dn_e}{dE_e} = \frac{K(E_e)}{r^2} \frac{\partial}{\partial r} \left[ r^2 \frac{\partial}{\partial r} \frac{dn_e}{dE_e} \right] + \frac{\partial}{\partial E_e} \left[ b(E_e) \frac{dn_e}{dE_e} \right] + Q(E_e) \quad (6)$$

Here,  $dn_e/dE_e$  is the number density of  $e^\pm$  per unit energy,  $K(E_e)$  is the diffusion parameter,  $b(E_e)$  is the rate of energy loss, and  $Q(E_e)$  the source term. We assume  $K(E_e) \equiv K_0(E_e/1\text{GeV})^\gamma$ , with  $K_0$  and  $\gamma$  specified in table 2, where scenario MAX maximizes the positron flux and MIN minimize it, and  $b(E_e) = -bE_e^2$  with  $b = 10^{-16}\text{GeV}^{-1}\text{s}^{-1}$ .

Table 2: *Different scenarios for diffusion parameters [42].*

| Scenario | $K_0$               | $\gamma$ |
|----------|---------------------|----------|
| MAX      | $1.8 \cdot 10^{27}$ | 0.55     |
| MED      | $3.4 \cdot 10^{27}$ | 0.7      |
| MIN      | $2.3 \cdot 10^{28}$ | 0.46     |

Assuming a power law injection, the solution of equation 6 is given by [41]

$$\frac{dn_e}{dE_e} = \frac{Q(E_e)}{\pi^{3/2}r^3} (1 - btE_e)^{\alpha-2} \left( \frac{r}{r_{diff}} \right)^3 e^{(r/r_{diff})^2} \quad (7)$$

where  $E < E_{max} \approx 1/(bt)$ , and by  $dn_e/dE_e = 0$  otherwise, with  $r_{diff}$  being

$$r_{diff} \approx 2 \sqrt{K(E_e)t \frac{1 - (1 - E/E_{max})^{1-\gamma}}{(1-\gamma)E/E_{max}}} \quad (8)$$

The local  $e^\pm$  flux from pulsars is fixed by pulsar distance  $r$ , the time of injection  $t$  which can be the pulsar age  $t = T$  for mature pulsars, and the normalization of the injected flux. In this way, the local flux is just  $J(E_e) = c(dn_e/dE_e)/(4\pi)$ . Figure 4 establishes energy spectra for different injection times  $t$  and two different diffusion scenarios (see tab. 2). From these figures, one can see that contributions from old pulsars can be negligible compared to young ones; at the same time, for young sources, the diffusion time limits the contribution. Moreover, one understands that propagation parameters are key for spectrum shape and intensity. Indeed, in the MED scenario (see tab. 2), contribution from low energy is relatively more important than for the MAX scenario, while the shape of the MAX energy spectra is more easily distinguishable than in the MED case. From the experimental detection point of view and in particular for AMS-02, it is clear that the MAX scenario is preferred because of the flux shape. In any case, having a strong cut-off at  $E_{max}$  could be a way to identify each pulsar contribution. The next sub-section will present the contribution in positron fraction of a sample of close-by pulsars.

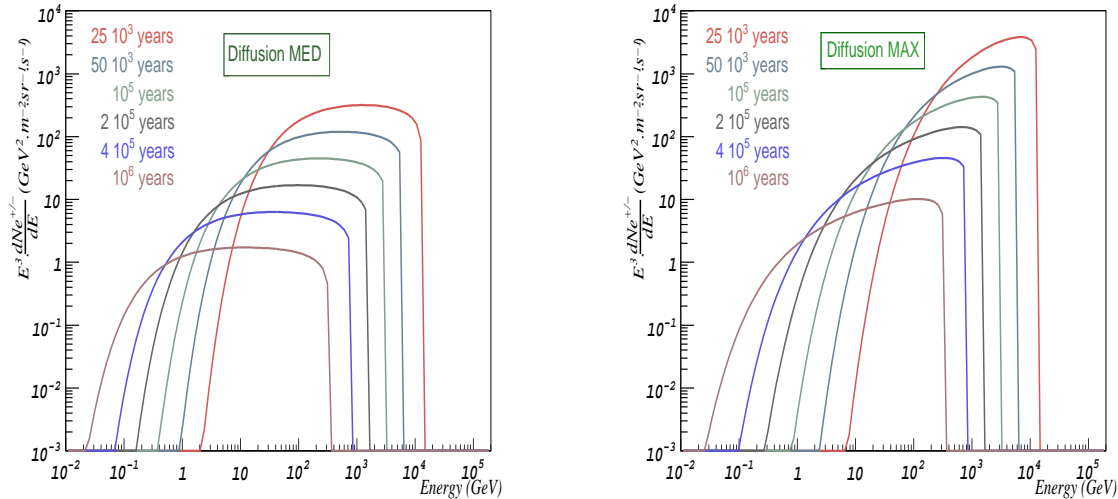


Figure 4: Energy spectra of electrons at different injection time from a source at  $r = 160$  pc,  $\alpha = 2$ , and  $E_{out} = 6 \cdot 10^{50}$  GeV for two diffusion scenarios: MED (left) and MAX (right) (see tab. 2).

## 2.2 Positron fraction from nearby pulsars

As experimental study, only the closest pulsars will be assumed as sufficient sources to explain the positron excess. In Table 3, additional data are given for the nearby pulsars of Table 1, where each one is assumed to have a pair production efficiency  $f_{e^\pm}$  that reproduces the PAMELA positron fraction in the three propagation scenarios of Table 2. Figure 5 illustrates the extreme cases, where a structure can be detected in the MAX scenario (left) and where none appears for the MIN scenario (right).

For these predictions, AMS-02 acceptance is taken to be  $\mathcal{A}_{e^\pm} = 0.045 m^2 \cdot sr$ . Further information on the AMS-02 electron/proton separation and its acceptance can be found in the literature [43] [44]. Two remarks can be made about AMS-02 electron acceptance. Firstly, below 10 GeV, the acceptance is lower than this mean value but the rate of cosmic rays is larger, so that the electron flux will still be high.

Table 3: *Data for selected nearby pulsars.*

| Name                 | $E_{tot}^{out}$<br>( $10^{50}$ GeV) | $f_{e^\pm}$ |       |       |
|----------------------|-------------------------------------|-------------|-------|-------|
|                      |                                     | (MAX)       | (MED) | (MIN) |
| Geminga [J0633+1746] | 74.                                 | 0.04        | 0.15  | 0.33  |
| Monogem [B0656+14]   | 9.                                  | 0.03        | 0.1   | 0.25  |
| Vela [B0833-45]      | 17.                                 | 0.03        | 0.1   | 0.25  |
| B0355+54             | 281.                                | 0.3         | 0.3   | 0.4   |
| Loop I [SNR]         | 43.                                 | 0.04        | 0.1   | 0.33  |

Secondly, at higher energies (above 500 GeV), the electron/proton separation will be more challenging for the detector, while at the same time the proton contamination is decreasing with energy, which could help to keep a good separation. For these reasons, the electron acceptance will be assumed energy-independent.

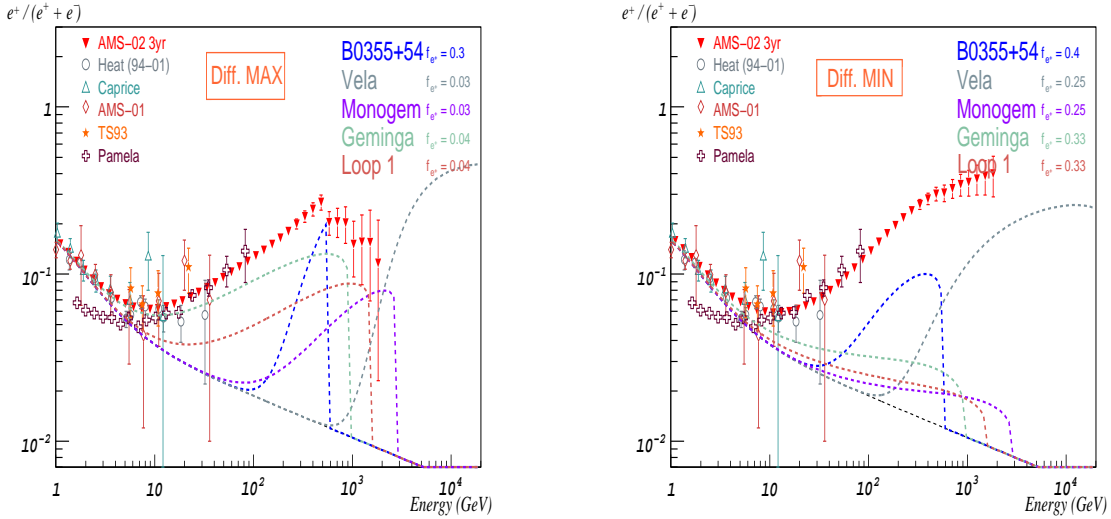


Figure 5: *Positron fraction reproduced by pulsar contributions for two propagation scenarios with AMS-02 capacity: MAX (left) and MIN (right) (see table 3).*

Using propagation scenario MAX, the pair production parameter  $f_{e^\pm}$  has reasonable values, up to a few percent (see Table 3), as expected by the models. In this scenario, pulsars with a large  $f_{e^\pm}$  (B0355+54 in our case) must appear like a peak in the spectrum, like seen in Figure 5 (left). On the other hand, the MIN scenario may smooth all contributions making almost impossible the pulsar distinction, and it implies important  $f_{e^\pm}$  indicating that pulsars couldn't be the unique contribution to this excess. To reproduce the positron excess in Figure 5 (right),  $f_{e^\pm}$  must be around 30 %, which means that almost one third of all the pulsar energy goes to electrons. About the MED scenario,  $f_{e^\pm}$  are reasonable but without pulsars distinction. To conclude, the MAX scenario is good enough for experimental detection, allowing low  $f_{e^\pm}$  and shape detection.

## 2.3 Positrons flux from pulsars continuum

Until now, only nearby pulsars had been considered to reproduce positron excess, from ATNF catalogue 184 more pulsars are "gamma-ray" type with an compatible age ( $Age \in [10^4, 60 \cdot 10^6]$  years) with energy range. Figure 6 (right) presented total contribution from all pulsars with the same  $f_{e^\pm} = 0.03$  compared to Geminga in the same condition. The whole faraway pulsars produce electrons like a Geminga, and pulsars continuum can be represented like a close one assuming some new pulsars could be discovered.

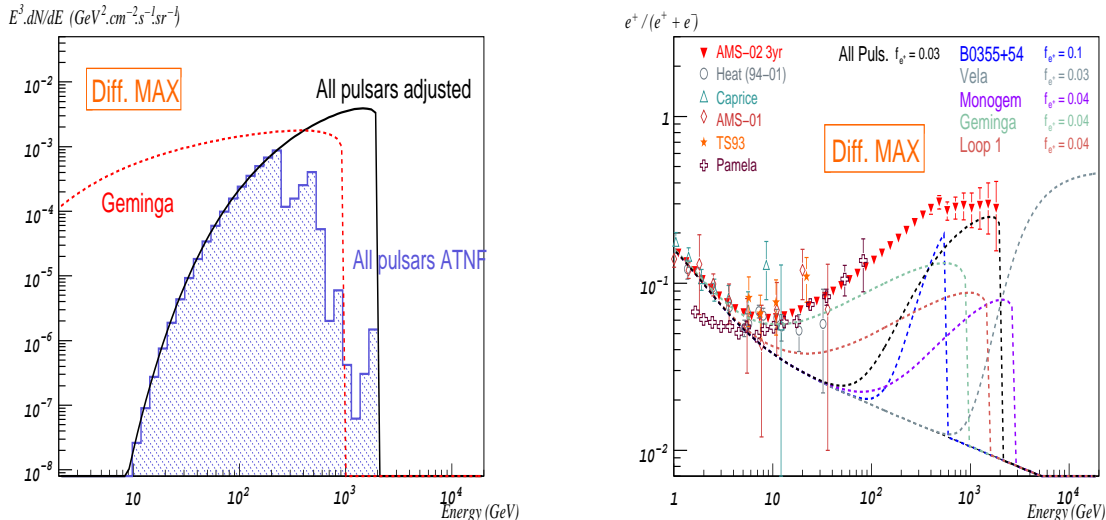


Figure 6: *Left: Electrons flux from all ATNF gamma-ray pulsars compared to Geminga with  $f_e^\pm = 0.03$ . Right: Positron fraction reproduced by nearby pulsars and far ones with AMS-02 capacity.*

Using the pulsars representation from figure 6 (left), a positron fraction is calculated in figure 6 (right) with conditions of figure 5 (left). For the MAX diffusion, pulsars faraway should diminish detector capacity to notice each pulsar.

## 3 Anisotropy: strong evidence for pulsar contribution?

The propagation of positrons-electrons does not allow to pinpoint each possible  $e^\pm$  source, reducing the chance of constraining, for example, which sources are responsible for the excess from dark matter. One possibility proposed by Mao & Shen [45] is that the closest pulsars can induce an anisotropy in the pulsars direction. Although propagation affects electron trajectory, close-by pulsars can induce a small dipole anisotropy, which should be present at sufficiently high energy [45].

### 3.1 Anisotropy in the $e^+e^-$ flux

In a very general way, the anisotropy of the  $e^\pm$  flux associated with diffusive propagation can be calculated as [46]

$$\delta = \frac{I_{max} - I_{min}}{I_{max} + I_{min}} = \frac{3K|\nabla(dN_e/dE_e)|}{c(dN_e/dE_e)} \quad (9)$$

where  $\nabla(dN_e/dE_e)$  is the gradient of  $e^\pm$  density. In the case of energy-independent diffusion anisotropy, Mao & Shen [45] proposed an estimation of the maximum expected anisotropy as

$$\delta_{max} = \frac{3}{2c} \frac{r}{t} \quad (10)$$

where  $r$  and  $t$  are respectively the distance and age of the pulsar. This simple relation forces us to choose not only the closest pulsars, but also young ones. Table 4 shows some expected energy-independent pulsar anisotropies. Vela being a young pulsar gives a strong anisotropy with respect to Geminga or Monogem.

Table 4: *Data for selected nearby pulsars.*

| Name                 | Dist. (pc) | Age (years)       | $\delta$ (%) |
|----------------------|------------|-------------------|--------------|
| Geminga [J0633+1746] | 160.       | $3.42 \cdot 10^5$ | 0.23         |
| Monogem [B0656+14]   | 290.       | $1.11 \cdot 10^5$ | 1.28         |
| Vela [B0833-45]      | 290.       | $1.13 \cdot 10^4$ | 12.5         |
| B0355+54             | 1100.      | $5.64 \cdot 10^5$ | 0.95         |
| Loop I [SNR]         | 170.       | $5.64 \cdot 10^5$ | 0.15         |

For energy-dependent diffusion, inserting Eq. 7 in 9, anisotropy can be expressed as

$$\delta = \frac{3}{2c} \frac{r}{t} \frac{(1-\gamma)E/E_{max}}{1 - (1 - E/E_{max})^{1-\gamma}} \frac{N_e^{Puls}}{N_e^{tot}} \quad (11)$$

where  $N_e^{Puls}$  and  $N_e^{tot}$  are  $e^\pm$  contribution from pulsars and from the electron background, taken from [40]. From the detection point of view, to observe an anisotropy at the  $5\sigma$  level, the observations must satisfy the condition  $\delta \geq 5\sqrt{2}/\sqrt{N_{evts}}$  where  $N_{evts}$  is the number of events collected. Figure 7 shows anisotropies expected for the two closest pulsars: Geminga and Monogem. These anisotropies are represented for two different propagation scenarios, MAX (left) and MIN (right), and compared to the sensitivity of the experiments PAMELA, Fermi-LAT and AMS-02. The sensitivity difference between experiments can be explained mainly by the electron acceptance: for Fermi-LAT it is  $\mathcal{A}_{Fer}^{e^\pm} \sim 1.5 - 2m^2 \cdot sr$  [11], for AMS-02 it is  $\mathcal{A}_{AMS}^{e^\pm} \sim 0.045m^2 \cdot sr$  [43], and for PAMELA,  $\mathcal{A}_{PAM}^{e^\pm} \sim 0.002m^2 \cdot sr$  [1].

Like in the positron fraction case (section 2.2), besides the  $f_{e^+}$  factor, the propagation affects the flux shape and therefore pulsar anisotropy, making Monogem unreachable for PAMELA and AMS-02 in the MAX configuration. Fermi-LAT would be able in any case to detect pulsar anisotropy. In the meantime, to prevent solar fluctuations and to reduce the uncertainties in anisotropy, it would be better to look for anisotropy above 10 GeV. In this case, only AMS-02 and Fermi-LAT will have sufficient sensitivity to discover an anisotropy at high energy. Unfortunately, both of them are not able to observe the flux decreasing.

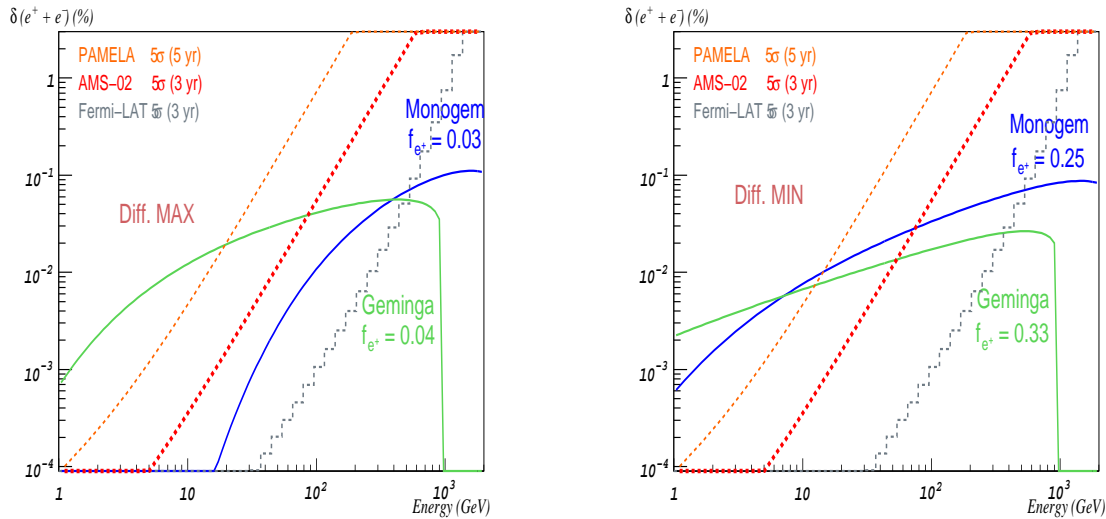


Figure 7: Anisotropy in  $e^\pm$  flux for Geminga and Monogem pulsars with sensitivity expected for AMS-02, Pamela and Fermi-LAT experiments for propagation scenario MAX (left) and MIN (right) (see table 3).

### 3.2 Anisotropy in $e^+$ flux: powerful detection

Analyzing positron flux is a direct way to probe the primary  $e^\pm$  source presented by Busching et al [47]. Anisotropy in  $e^+$  flux is the best way to characterize a close-by source and to constrain it. Fermi-LAT can not perform this study, because it is not able to separate positrons from electrons. AMS-02 with its superconductor magnet having a bending power of  $0.86 T \cdot m^2$  [48], will differentiate between electrons and positrons above 300 GeV. The study performed with  $e^\pm$  can be applied to  $e^+$ , and figure 8 present the results for two propagation sets: MAX (left) and MIN (right). AMS-02 should detect anisotropy above 10 GeV for all propagation scenarios, if pulsars are the only component of the positron excess.

### 3.3 Discussion on anisotropy detection

In last section, Geminga and Monogem were supposed to be sufficiently distant to induce an individual dipole. Nevertheless, according particles propagation and the two pulsar galactic coordinates,  $Monogem = (201.11^0, +08.25^0)$  and  $Geminga = (195.13^0, +04.27^0)$ , measured anisotropy can be assumed the sum of the two contributions. Looking at figures 7 and 8, the two contributions sum should be more important at low energy with MIN scenario as figure 9 (left) shows, allowing detection for all the experiments.

An another hypothesis can be discussed, faraway pulsars (section 2.3) can be added to the standard electron-positron background. Assuming the propagation sufficiently diffusive to produce an isotropic contribution, Geminga and Monogem anisotropy can be estimated with this new background in figure 9 (right). The greatest effect is expected at high energy, keeping same anisotropy below 100 GeV. To conclude, anisotropy from Geminga and Monogem can be added improving detection, and pulsar background should not affect anisotropy measurement.

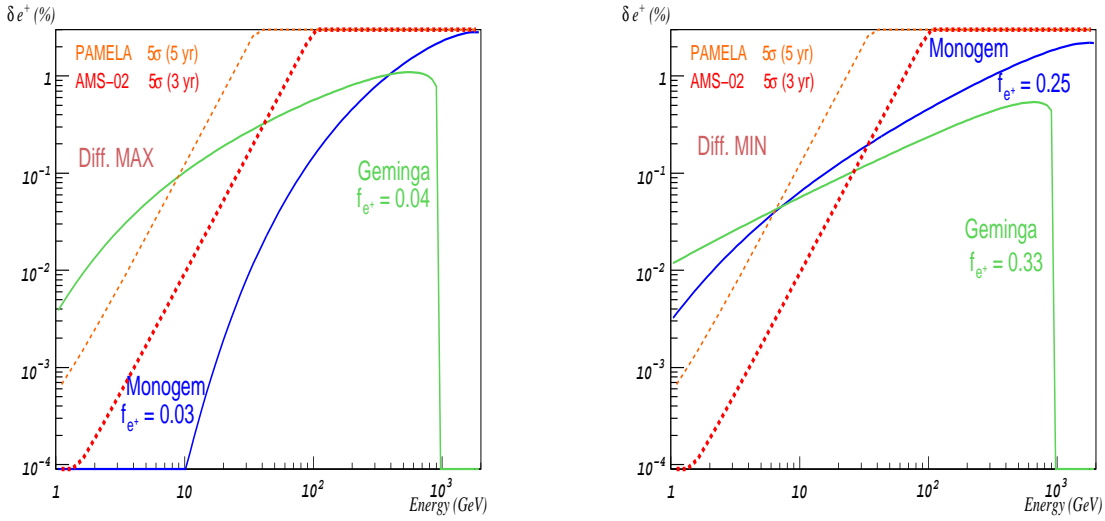


Figure 8: Anisotropy in  $e^+$  flux for Geminga and Monogem pulsars with sensitivity expected for AMS-02 and Pamela experiments for propagation scenario MAX (left) and (right) (see table 3).

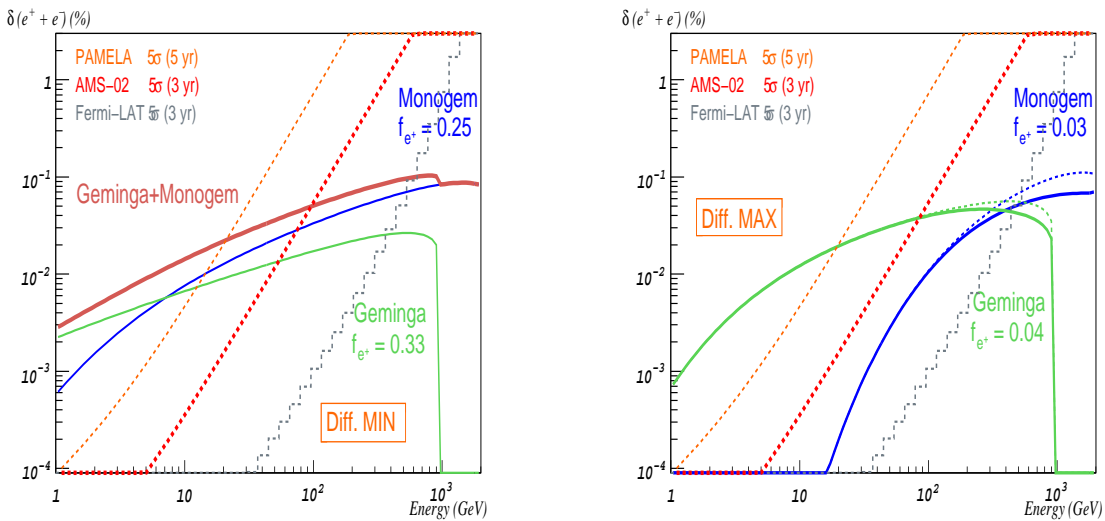


Figure 9: Left: Anisotropy in  $e^\pm$  flux for sum of Geminga and Monogem contributions for MIN diffusion. Right: Geminga and Monogem with pulsars background (line) and without (dashline) for MAX diffusion with sensitivity expected for PAMELA, AMS-02 and Fermi-LAT.

## Conclusion

For three years, positron fraction is studied with new generation experiments, PAMELA had confirmed the increase of positrons above 10 GeV and Fermi-LAT has observed electrons flux above standard background. Next years, AMS-02 will provide a positron fraction at higher energy with better accuracy, and Fermi-LAT will extend his energy range from GeV to TeV. In this article, we considered that positrons flux is the result of electron-positron pairs production in nearby pulsars,

and different propagation scenarios were studied. The case which maximizes electrons flux (MAX) is preferred for experimental detection, with a possibility to separate each pulsar contribution in AMS-02. In agreement with models, this parameters set implies low pair production parameters for pulsars. The others propagation parameters sets will not allow to distinguish each pulsar, and for the one minimizing positron flux (MIN), pulsars should not be able to produce the whole extra contribution. Without pulsar distinction, anisotropy in the positron and/or positron-electron flux will be a powerful test to establish pulsar contribution. Geminga and Monogem should induce enough anisotropy to be detected in three years with  $5\sigma$  significance by Fermi-LAT and AMS-02. Propagation will be constraint by AMS-02 measurement mainly with  $Be^{10}/Be^9$  and  $B/C$  ratio.

## References

- [1] **PAMELA experiment** <http://pamela.roma2.infn.it>
- [2] **Fermi-LAT experiment** <http://www-glast.stanford.edu>
- [3] **S. Barwick et al.** *Nucl. Inst. & Med.*, 400 (1997) 34
- [4] **AMS-02 experiment** <http://ams.cern.ch>; <http://ams.nasa.gov>
- [5] **Golden et al.** *ApJ*, 457 (1996), L103
- [6] **Ma Duvernois et al.** *ApJ*, 559 (2001), 296-303
- [7] **S. Barwick et al.** *Phys. Rev. Lett.*, 75 (1995) 390; *ApJ*, 482 (1997) L191
- [8] **Boezio et al.** *ApJ*, 532 (2000), 653
- [9] **Alcaraz et al.** *Phys. Lett. B*484 (2000) 10
- [10] **O. Adriani et al.** *Nature* 458, (2009) 607-609
- [11] **A.A. Abdo et al.** *Phys. Rev. Lett.* 102 (2009) 181101
- [12] **J. Chang et al.** *Nature* 456, (2008) 362-365
- [13] **H.E.S.S collaboration** *Phys. Rev. Lett.* 101 (2008) 261104
- [14] **I.V. Moskalenko and A.W. Strong** *ApJ*, 493 (1998a) 694
- [15] **D. Maurin et al.** *arXiv:astro-ph/0212111*
- [16] **J.H. Taylor and D.R. Stinebring** *ARA&A* 24 (1986) 285
- [17] **D.C. Backer** *Pulsars (Galactic and Extragalactic Radio Astronomy, 1988)* pp. 480-521
- [18] **M. Cirelli and A. Strumia** *arXiv:0808.3867* (2008)
- [19] **L. Bergstrom et al.** *arXiv:0808.3725* (2008)
- [20] **J. Zhang et al.** *arXiv:0812.0522* (2008)
- [21] **D. Grasso et al.** *arXiv:0905.0636* (2009)
- [22] **A. Hewish et al.** *Nature* 217 (1968) 709
- [23] **ATNF catalogue** <http://www.atnf.csiro.au/research/pulsar/psrcat/>
- [24] **M.A. Rudermans and P.G. Sutherland** *ApJ*, 196 (1975) 51
- [25] **J. Arons** *ApJ*, 266 (1983) 215A
- [26] **K. Cheng et al.** *ApJ*, 300 (1986) 522C; *ApJ*, 300 (1986) 500C;

- [27] **D.J. Thompson et al.** *ApJ*, 436 (1994) 229
- [28] **J.M Fierro et al.** *ApJ*, 447 (1995) 807
- [29] **P. Goldreich and W.H. Julian** *ApJ*, 157 (1969) 869
- [30] **X. Chi et al.** *ApJ*, 459 (1996) L83
- [31] **L. Zhang & K.S. Cheng** *ApJ*, 487 (1997) 370
- [32] **R.N. Manchester et al.** *ApJ*, 129 (2005) 1993
- [33] **M.S Longair** "High Energy Astrophysics", Vol II, Cambridge University Press, 2nd edition (1994)
- [34] **F.A. Aharonian et al.** *A&A* 294 L41-L44 (1995)
- [35] **D. Hooper et al.** *JCAP* 0901 (2009) 025.
- [36] **Stefano Profumo** *arXiv:0812.4457*
- [37] **J.K. Daugherty and A.K. Harding** *ApJ*, 252 (1982) 337
- [38] **X. Chi et al.** *ApJ*, 459 (1996) L83
- [39] **L. Zhang & K.S. Cheng** *A&A*, 368 (2001) 1063
- [40] **Barwick et al.** *ApJ*, 498 (1998) 779
- [41] **A.M. Atoyan et al.** *Phys. Review D*, vol. 52, num. 6 (1995)
- [42] **T. Delahaye et al.** *Phys. Rev. D* 77 063527 (2008), 0712.2312
- [43] **J. Pochon** *PhD. thesis (2005):* <http://tel.archives-ouvertes.fr/tel-00010164/fr>
- [44] **P. Maestro** *PhD. thesis (2003):* <http://ams.cern.ch/AMS/Reports/AMSnotes2003>
- [45] **C.Y. Mao et C.S. Shen** *Chinese Journal Phys.* vol. 10 no. 1 (1972)
- [46] **P. Ginzburg & S.I. Syrovatskii** *The Origin of Cosmic Rays (1964) N.Y. Macmillan*
- [47] **I. Bsching et al.** *ApJ*, 678 (2008) L39, 0804.0220
- [48] **AMS-02 Collaboration** *Nucl. Instrum. Meth. A* 588 (2008) 227-234